The subtle role of heteroaromatics in the second-order susceptibility in a series of amphiphilic styryl dye Langmuir–Blodgett films

Jie Zheng,[a] Chun-Hui Huang,*[a] Yan-Yi Huang,[a] Deng-Guo Wu,[a] Tian-Xin Wei,[a] An-Chi Yu[b] and Xin-Sheng Zhao[b]

[a] State Key Laboratory of Rare Earth Materials Chemistry and Applications, Peking University—The University of Hong Kong Joint Laboratory in Rare Earth Materials and Bioinorganic Chemistry, Peking University, Beijing 100871, China
[b] Department of Chemistry, Peking University, Beijing 100871, China

A series of amphiphilic styryl dyes: 2-(4-dihexadecylaminostyryl) benzothiazole methiodide (BTM), 2-(4-dihexadecylaminostyryl) benzoxazole methiodide (BOM), and 2-(4-dihexadecylaminostyryl) benzimidazole methiodide (BIM), were synthesized; their monolayers were successfully deposited on quartz slides by the Langmuir–Blodgett technique and formed H aggregates. Second-order susceptibilities $\chi^{(2)}_{zzz}$ of the monolayers were determined with a polarized laser beam (Nd : YAG, $\lambda = 1.064$ μm). The values of $\chi^{(2)}_{zzz}$ are 215, 132, and 67 pm V^{-1} for BTM, BOM and BIM, respectively. Charge distributions over the entire molecules for the dye models were calculated using the MINDO/3 method in the MOPAC 7.0 program. Experimental data and semiempirical quantum chemical calculation results show that electron deficiencies of the heteroaromatic rings play an important role in determining the second harmonic generation of organic dye LB films.

The need for information technologies such as telecommunication, optical computing, and information storage promotes the rapid development of research on nonlinear optical (NLO) materials.[1] Organic NLO materials have attracted considerable attention owing to their large second harmonic responses, good tailorability, and processibility.[2–10] A general strategy for designing organic nonlinear optical materials is to introduce donor and acceptor group on different ends of a π-electron conjugated bridge (D–π–A), which meets the requirements for second harmonic generation (SHG): asymmetry and effective redistribution of electric charge through the conjugated bridge in the excited state.[2–5] Although a benzene ring is generally used as a conjugated bridge unit to connect donor and acceptor, its high aromatic delocalization energy hinders efficient intramolecular charge transfer between the donor and acceptor, resulting in the reduction or saturation of SHG values.[8–10] Recent work indicates that introduction of heteroaromatic rings into the conventional homocyclic D–π–A conjugated systems can lead to large enhancement of second harmonic response due to the lower delocalization aromatic energy of heterocycles relative of homocycles.[8–11] It is known that the properties of heteroaromatics can be manipulated by just changing the heteroatoms,[12–14] thus it appeared very interesting to study the effects of different heteroatoms on the SHG signal of Langmuir–Blodgett (LB) films.

In this paper, we report the synthesis of a series of amphiphilic dyes with the same donor and conjugated bridge but different acceptors: 2-(4-dihexadecylaminostyryl) benzothiazole methiodide (BTM), 2-(4-dihexadecylaminostyryl) benzoxazole methiodide (BOM), and 2-(4-dihexadecylaminostyryl) benziminazole methiodide (BIM). The second harmonic response of these three dyes as LB monolayers was measured. The similarity in structures for the three dyes provides a possibility to study the effect of heteroatoms (S, O or N atom) in the acceptor fragment on the SHG in LB films.

Experimental

Materials and apparatus

2-Methylbenzothiazole, 2-methylbenzoxazole and 2-methylbenzimidazole were purchased from Aldrich and used as received. Other reagents were AR grade. Water used was deionized water purified by passing through an EASY pure R-F compact ultrapure water system (18 MΩ).

Elemental analyses were carried out on a Carlo Erba 1102 and a Heraeus CHN-Rapid instrument. ^{1}H NMR spectra were measured using a Bruker ARX400 NMR spectrometer with tetramethylsilane as an internal standard (in CDCl$_3$). UV-Vis spectra were recorded by using Shimadzu UV-3100 spectrometer. Films were formed and deposited on quartz by using a Langmuir trough (Nima Technology Model 622).

Synthesis of target compounds

The target amphiphilic styryl dyes were obtained by condensing their methyl azolium precursors with 4-dihexadecylaminobenzaldehyde, (Scheme 1).[6] The products were purified by column chromatography on silica gel with a mixed (1 : 1) solvent of chloroform and light petroleum (30–60 °C) as eluent. Their structures were confirmed by elemental analysis and ^{1}H NMR.

BTM. Mp: 171 °C. Elem. anal.: Found: C: 68.10, H: 9.94, N: 3.17%. Calc. for $C_{48}H_{79}SN_2I$: C: 68.40, H: 9.38, N: 3.32%. ^{1}H NMR (CDCl$_3$): 0.877 (t, 6H, 2 CH$_3$), 1.26 (m, 52H, 26 CH$_2$), 1.58 (t, 4H, 2 CH$_2$), 3.27 (t, 4H, 2 CH$_2$N), 4.33 (s, 3H, R$_3$–N$^+$–CH$_3$), 6.49 (d, 1H, –CH=CH), 6.54 (d, 1H, –CH=CH), 7.45 (d, 2H, ArH), 7.51 (m, 1H, ArH), 7.66 (d, 1H, ArH), 7.78 (d, 1H, ArH), 7.86 (m, 1H, ArH), 8.04 (d, 2H, ArH).
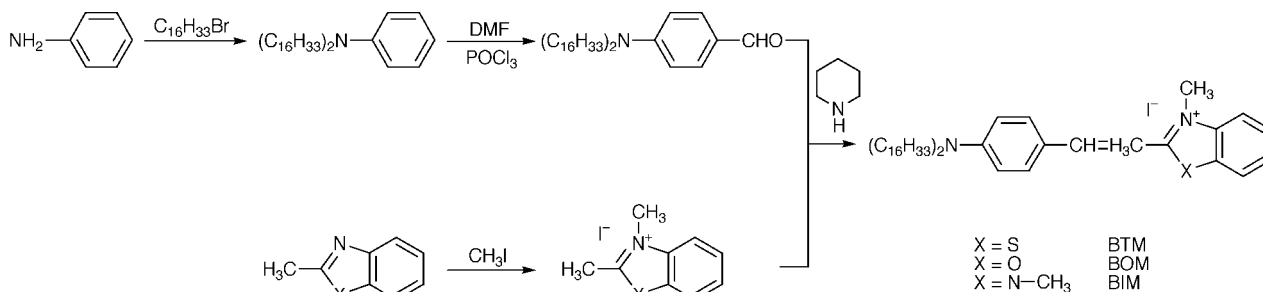
Scheme 1 The common synthetic route for the styryl dyes.

BOM. Mp: 168 °C. Elem. anal.: Found: C: 69.5, H: 9.43, N: 3.12% Calc. for $C_{48}H_{79}ON_2I$: C 69.7, H: 9.56, N: 3.38%, ^{1}H NMR(CDCl3): 0.87 (t, 6H, 2 CH_3), 1.24 (m, 52H, 26 CH_2), 1.70 (t, 4H, 2 CH_2), 3.22 (t, 4H, 2 CH_2N), 4.48 (s, 3H, R_3–N^+–CH_3), 6.94 (d, 1H, –CH=CH), 7.06 (d, 1H, –CH=CH), 7.52 (d, 2H, ArH), 7.69 (m, 1H, ArH), 7.80 (d, 1H, ArH), 8.18 (d, 1H, ArH), 8.31 (m, 1H, ArH), 8.83 (d, 2H, ArH).

BIM. Mp: 163 °C. Elem. anal.: Found: C: 69.5, H: 10.1, N: 4.68% Calc. for $C_{49}H_{82}N_3I$: C 70.05, H: 9.84, N: 5.00%. ^{1}H NMR(CDCl3): 0.878 (t, 6H, 2 CH_3), 1.259 (m, 52H, 26 CH_2), 1.558 (t, 4H, 2 CH_2), 3.24 (t, 4H, 2 CH_2N), 3.90 (s, 3H, R_3–N^+–CH_3), 4.19 (s, 3H, R_3–N^+–CH_3), 6.45 (d, 1H, –CH=CH), 6.77(d, 1H, –CH=CH), 7.35(d, 2H, ArH), 7.54 (m, 1H, ArR), 7.63 (d, 1H, ArH), 7.64 (d, 1H, ArH), 7.78 (m, 1H, ArH), 7.81(d, 2H, ArH).

π–A isotherm and film deposition

Samples of the dyes in chloroform solution (0.24–0.3 mg ml^{-1}) were spread onto a water subphase (pH 5.6) at 20 °C. After evaporation of the solvent, the monolayers were compressed at a speed of 80 cm^2 min^{-1} and then were transferred at an up rate of 5 mm min^{-1}, under surface pressure of 30 mN m^{-1}, onto the quartz slides, which were hydrophilically pretreated following the usual way.[9] The films with transfer ratios ca. 1.0 ± 0.1 were used in further experiments.

SHG measurements

The SHG measurements were performed in transmission geometry using a Y-type quartz plate (d_{11} = 0.5 pm V^{-1}) as a reference and with a Q-switched Nd : YAG laser (1.064 μm). A 1/2λ plate and a Glan–Taylor polarizer were used to vary the polarization direction of the laser beam. The laser light, linearly polarized either parallel (p) or perpendicular (s) to the plane of incidence, was directed at an incidence angle of 45° onto vertically mounted samples. A set of 1.064 μm filters and a monochromator were used to ensure that the signal detected by the photomutiplier was the second-harmonic radiation generated by the films. The average output signal was recorded on a digital storage oscilloscope (HP54510). All the reported SHG data are averaged values of at least three separate measurements.

Semiempirical quantum calculations

In the present work, AM1 in the program system MOPAC 7.0 was used to optimize the geometric structures of the dye congener cations. MINDO/3 in the program system MOPAC 7.0 was used to calculate the net charges of the atoms in the cations. The charge distribution in one fragment is obtained by summing the net charges of the atoms in the fragment.

Results and discussion

Pressure–area isotherms

The surface pressure–area (π–A) isotherms for the three styryl dyes at the air–water interface are shown in Fig. 1. The iso-

therm traces of the dyes can be divided into three regions: gas (G) phase, liquid-expanded (LE) phase, and liquid-condensed (LC) phase, in terms of a typical scheme for the behavior of long-chain amphiphilic molecules at the air–water interface.[15] The characteristic values obtained from the π–A isotherms are summarized in Table 1. It can be clearly seen that the transition pressures from the LE to LC phase for the dyes are distinctive. This could be attributed to the different H-bond forming abilities of S, O and N atoms. During this phase transition, the chromophores lift from the water surface with increasing compression, thus a higher compression pressure is required for compounds with heteroatoms that can form stronger H-bonds with water. The weaker H-bond forming ability of the S atom allows BTM to transit into the LC phase at lower pressure and form a highly oriented monolayer in the LC phase at the water surface. A short range or absence of the intermediate LE phase was also observed in other systems.[16] The isotherm of BOM is more similar to many straight long-chain urea and acid systems, in which H-bonding has a great effect on the isotherms.[17] The rapid rise in surface pressure to ∼50 mN m^{-1} indicates that the three dyes have good film-forming abilities. The limiting surface area can be obtained by extrapolating the slopes in the condensation region to zero surface pressure, which gives 53, 47 and 72 Å^2 for BTM, BOM and BIM, respectively. The larger limiting area for BIM is ascribed to its extra methyl group, which not only occupies
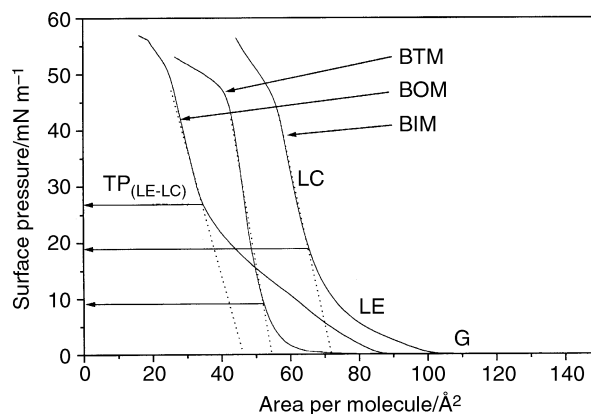
Fig. 1 Surface pressure-area isotherms of BTM, BOM and BIM at the air–water interface (20 ± 1 °C).

Table 1 Transition pressures (LE–LC), collapse pressures, surface limiting areas per molecule of the styryl dyes (20 ± 1 °C)

| Dye	TP$_{(E-C)}$[a]/mN m^{-1}	Collapse pressure/mN m^{-1}	Limiting area/Å^2
BTM	8	45	53
BOM	18	49	47
BIM	27	47	72

[a] Transition pressure from liquid-expanded phase to liquid-condensed phase.

a certain area, but also could prohibit the aggregation of BIM dye molecules, leading to the larger limiting area than others. The smaller limiting area for BOM may be attributed to the good H-bond forming ability of the O atom, which can make the chromophores of BOM pack more closely than those of BTM do. It is known that the limiting area values for simple long-chain carboxylic acids are in the range of 18–25 Å² per molecule,[16,17] thus the larger values obtained for the dyes suggest that the large bulky head groups determine the packing density in the monolayers.

UV-Vis spectra

Fig. 2(*A–C*) shows the UV-Vis spectra of the three dyes under different conditions (in chloroform, ethanol and as LB monolayers). Several conclusions can be drawn from the data. First, compared to the spectra in chloroform solution, the maximum absorption wavelengths of the dye films on the quartz substrates are blue-shifted 100, 61 and 3 nm for BTM, BOM and BIM, respectively. Such blue shifts result from
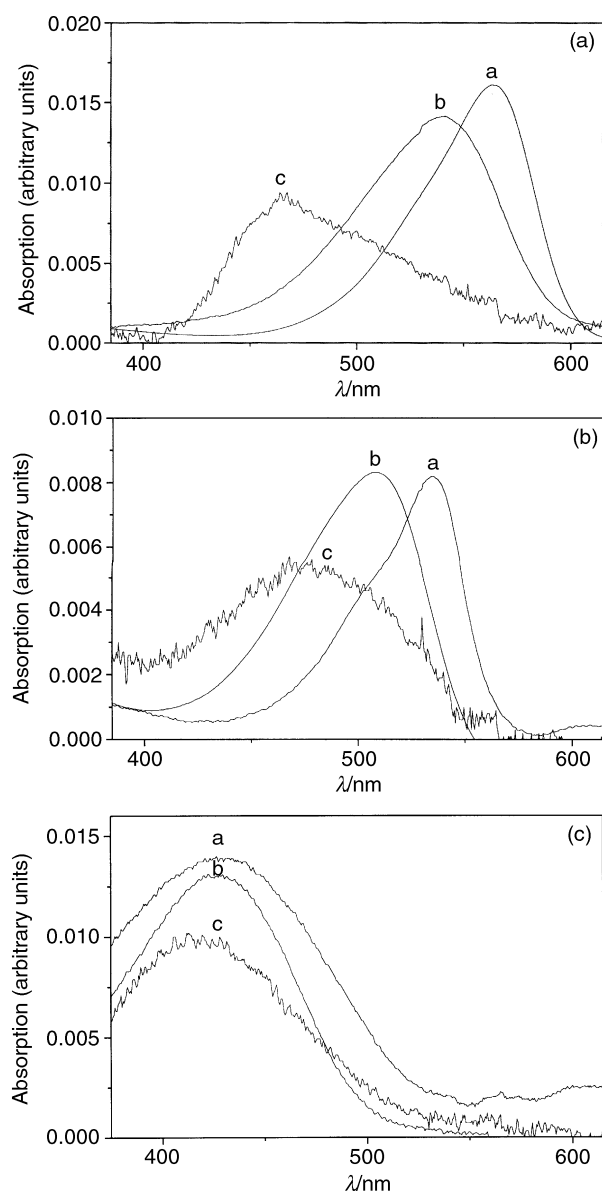
Fig. 2 UV-Vis spectra of (*a*) BTM (curve *a*) $\lambda_{max} = 564$ nm in chloroform, (curve *b*) $\lambda_{max} = 539$ nm in ethanol, (curve *c*) $\lambda_{max} = 464$ nm as a LB monolayer; (*b*) BOM (curve *a*) $\lambda_{max} = 534$ nm in chloroform, (curve *b*) $\lambda_{max} = 509$ nm in ethanol, (curve *c*) $\lambda_{max} = 473$ nm as a LB monolayer; (*c*) BIM (curve *a*) $\lambda_{max} = 429$ nm in chloroform, (curve *b*) $\lambda_{max} = 426$ nm in ethanol, (curve *c*) $\lambda_{max} = 426$ nm as a LB monolayer.

intermolecular dipole–dipole interactions of chromophores and indicate that the chromophores pack together in a "head-to-head" manner to form H aggregates on the substrates.[18,19] The smallest blue shift (3 nm), observed for BIM, may be due to a the weaker interaction between its chromophores, because the external methyl groups increase the distance between the choromophores and decrease their interactions, which is in agreement with the larger limiting area for BIM. Second, comparison of the UV-Vis spectra of the dyes in ethanol solution (a more polar solvent) with those in chloroform solution indicates that the maximum absorption wavelengths (λ_{max}) for all the dyes are blue-shifted 25, 25 and 3 nm for BTM, BOM and BIM, respectively. Such blue shifts suggest that the dipole moments in the excited state are smaller than those in the ground state for all the dyes.[20]

Second-order susceptibilities of the dye films

With the assumptions that the chromophores have a common tilt angle φ with respect to the normal of the film surface, with a random azimuthal distribution, and that the monolayer thickness is 3 nm for all the dyes, as calculated from the length of the molecules, the SHG data from the LB films were analyzed using general procedure described by Ashwell *et al.*[21]

The SHG properties of the three dyes are shown in Table 2. It can be seen that the values of φ for BTM, BOM and BIM are 43°, 48° and 46°, which suggests that the orientation of chromophores in the films change with different the heteroatoms. The $\chi^{(2)}_{zzz}$ values of the dyes are far larger than that of a homocylic dye with a similar structure: the iodide salt of octadecyl-4-[2-(4-dibutylaminophenyl)ethenyl] quinolinium [120 pm V^{-1} (20 layers)],[21a] suggesting that the introduction of heterocycles can increase the second harmonic response greatly.
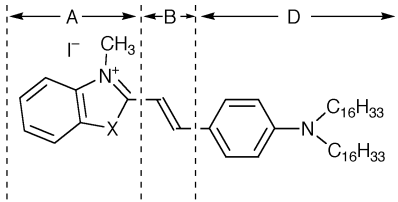
On another common assumption for organic materials that the molecular hyperpolarizability (β) is dominated by the component along the intramolecular donor–π–acceptor axis, β values of the dyes can be calculated from the $\chi^{(2)}_{zzz}$ values of dye monolayers using the following equation:[6,21]

$$\chi^{(2)}_{zzz} = N f_{2\omega}(f_\omega)^2 \beta_{zzz} \cos^3\varphi$$

in which N is the number of molecules per unit volume and $f_{\omega, 2\omega} = (n_{\omega, 2\omega} + 2)/3$ is a local field correction factor, where n_ω and $n_{2\omega}$ are the refractive indexes of the film at the fundamental and second-harmonic frequencies, respectively. In this treatment n is taken to be $n_\omega \approx n_{2\omega} = 1.5$ for BIM and $n_\omega = 1.5$, $n_{2\omega} = 1.8$ for BTM and BOM, due to the partial resonance absorption of BTM and BOM LB films with the second harmonic wavelength ($\lambda_{2\omega} = 532$ nm).[6,21] The large blue shifts (68 and 59 nm) for BTM and BOM monolayers are favorable to decrease the errors due to resonance absorption. Although this assumption may be questionable for an exact evaluation of data, it can minimize the effects due to different film-forming properties such as different limiting areas and φ angles on the SHG, and offers a convenient simplification of the data analysis for comparison to many different compounds with similar structure.[6] It can be seen from Table 2 that molecular hyperpolarizabilities (β_{zzz}) for the dyes follow the same order as their $\chi^{(2)}_{zzz}$ values: BTM > BOM > BIM. The coincidence in the orders of β_{zzz} and $\chi^{(2)}_{zzz}$ stimulated us to study the effect of heteroatoms on NLO-active properties more thoroughly.

Relationship between SHG and heterocycles in the acceptor fragment

Because of the distinct electronic configuration of heteroatoms, introduction of different heteroatoms inevitably affects the aromatic delocalization energies of molecules and changes their electron density distributions.[12–14] The similarity in the

Table 2 SHG properties[a] of the styryl dyes and the calculated positive charge distributions on the donor, acceptor and bridge fragments

The congeners of the dyes: X = S, O, N—CH$_3$

Dye	$I^{\text{p-p}}$	$I^{\text{s-p}}$	$\chi_{\text{eff}}^{(2)}/$ pm V^{-1}	$\chi_{zzz}^{(2)}/$ pm V^{-1}	$\chi_{zxx}^{(2)}/$ pm V^{-1}	$\varphi/°$	$\beta_{zzz}/10^{-30}$ esu	$\beta_{xzz}/10^{-30}$ esu	Charge distribution in the congeners A	B	D
BTM	3138	452	174	215	93	43	609	263	0.73	0.03	0.22
BOM	1818	335	133	132	81	48	360	221	0.69	0.07	0.24
BIM	386	68	61	67	36	46	270	145	0.65	0.06	0.29

[a] I is the intensity of the values of $\chi^{(2)}$ obtained by measuring monolayers of the dyes under the same conditions. $I_{\text{quartz}} = 259\,978\,4.5$. φ is the tilt angle with the substrate normal of the chromophore in a LB film.

structures of the dyes simplifies the problem and provides an easier way to clarify these two effects of heterocycles on the SHG.

Lower aromatic delocalization energy. It is known that when isolated p orbitals overlap to form π orbitals, the total energy can decrease to make the system more stable. This difference in total energies is called the external stabilization energy, also known as the aromatic delocalization energy for aromatic compounds.[12,13] Recent studies indicated that the introduction of different heteroatoms had distinctive effects on the decrease of the aromatic delocalization energy.[13] For example, recent theoretical computations on a set of five-membered C$_4$H$_4$X ring systems with 6π electrons indicated that the aromatic delocalization energy of five-membered monocyclic heterocycles decreases in the order: pyrrole > thiophene > furan.[14] There is much the same trend of aromatic delocalization energy in the imidazole-thiazole-oxazole series as in the pyrrole-thiophene-furan series;[13] thus, it can be safely concluded that the sequence of delocalizaton energy for the present system is BIM > BTM > BOM. However, if aromatic delocalization energy is the only factor in determining the SHG, in other words, the lower the delocalization energy, the higher the second harmonic response, the order in SHG of the present system should be BOM > BTM > BIM. Such sequence is different from the experimental results (BTM > BOM > BIM). Thus, the strength of the acceptor must also be considered.

Electron deficiency of the acceptors. The strength of an acceptor is directly related to its electron deficiency. Increasing the electron deficiency of an acceptor is an efficient way to enhance the second harmonic response.[7] It is known that neutral azoles, a ring containing two heteroatoms (such as thiazole, oxazole and imidazole), are electron deficient in terms of the electron density on the carbons in the rings; their electron deficiencies decrease in the order: thiazole > oxazole > imidazole.[14] In the title systems with a D–π–A structure, the electron deficiencies of the acceptors increase greatly compared with their neutral counterparts when the common nitrogen atom in the acceptor is quaternized.

To further study the order of electron deficiency in this azolium system, while neglecting the interaction of molecules on the film, positive charge distributions on the different parts of three model molecules of the dye congeners: 2-(4-dimethyl-aminostyryl) benzothiazole methiodide CBTM, 2-(4-dimethyl-aminostyryl) benzoxazole methiodide CBOM and 2-(4-dimethylaminostyryl) benzoiminazole methiodide CBIM, were calculated using the AM1 and MINDO/3 methods in the MOPAC 7.0 program. The results are presented in Table 2. It can be seen that the order of positive charge density on the acceptor fragment is CBTM > CBOM > CBIM, which follows the sequence of electron deficiency of the neutral azoles. This ordering of electron deficiency for the dyes coincides with their SHG response order, suggesting that the electron deficiency of the acceptor plays a more important role in the SHG than its aromatic delocalization energy. The calculated results are also in agreement with the experimental observations: with the increase of acceptor strength, the maximum absorption of the dyes in chloroform solution is red-shifted, going from 429 nm for BIM, 534 nm for BOM, to 564 nm for BTM. It is known that the maximum absorption in the visible region is assigned to the intramolecular charge-transfer transition (ICT), which is usually regarded as a semi-empirical tool to predicate the trend of β values in compounds with electronically similar structures.[9] Consequently, the red shifts of ICT in the presented systems with electronically similar structures suggest that the decrease in the energy difference between the first excited state and the ground state leads to more effective charge transfer between the donor and the acceptor groups, as well as contributing to the enhancement of the second-order susceptibility with the change of heteroatom from N, to O, to S.

Conclusions

A class of amphiphlic styryl dyes with similar structures but containing different heteroatoms in the acceptor fragment was synthesized. These different heteroatoms have a great effect on the film-forming properties and second harmonic responses of dye monolayers. The second-order susceptibilities of the dye monolayers increase in the order: BIM < BOM < BTM. The different effects of heteroatoms in the acceptor on SHG provide a strategy for designing new NLO materials.

Acknowledgements

References

1   A. Miller, K. R. Welford and B. Daino, *Nonlinear Optical Materials and Devices for Applications in Information Technology*, Kluwer Academic Publishers, The Netherlands, 1993.

2   D. S. Chemla and J. Zyss, *Nonlinear Optical Properties of Organic Molecules and Crystals*, Academic Press, New York, 1987, vol. 1–2.

3   D. M. Burland, R. D. Miller and C. A. Walshy, *Chem. Rev.*, 1994, **94**, 31.

4   S. R. Mader, D. N. Beratan and L.-T. Cheng, *Science*, 1991, **252**, 103.

5   C. A. Mirkin and M. A. Ratner, *Annu. Rev. Phys. Chem.*, 1992, **43**, 719.

6   C. Bubeck, A. Laschewsky, D. Lupo, D. Neher, P. Ottenbreit, W. Prass, H. Ringsdorf and G. Wenger, *Adv. Mater.*, 1991, **3**, 54.

7   (*a*) T.-R. Cheng, C.-H. Huang, L.-B. Gan, C.-P. Luo, A.-C. Yu and X.-S. Zhao, *J. Mater. Chem.*, 1998, **8**, 931; (*b*) C. H. Huang, K. Z. Wang, G. X. Xu, X. S. Zhao, X. M. Xie, Y. Xu, Y. R. Liu, L. G. Xu and T. K. Li, *J. Phys. Chem.*, 1995, **99**, 14397; (*c*) L. H. Gao, K. Z. Wang, C. H. Huang, X. S. Zhao, X. H. Xia, T. K. Li and J. M. Xu, *Chem. Mater.*, 1995, **7**, 1047.

8   C. W. Dirk, H. E. Katz and M. L. Schilling, *Chem. Mater.*, 1990, **2**, 700.

9   (*a*) K. Y. Wong, A. K. Y. Jen, V. P. Rao and K. J. Drost, *J. Chem. Phys.*, 1994, **100**, 6818; (*b*) L.-T. Cheng, W. Tam, S. H. Stevendon, G. R. Meredith, G. Rikken and S. R. Marder, *J. Phys. Chem.*, 1991, **95**, 10631; (*c*) V. Keshari, W. M. K. P. Wijekoon, P. N. Prasd and S. P. Karna, *J. Phys. Chem.*, 1995, **99**, 9045; (*d*) A. K.-Y. Jen, V. P. Rao, K. Y. Wong and K. J. Drost, *J. Chem. Soc., Chem. Commun.*, 1993, 90.

10 I. D. L. Albert, T. J. Marks and M. A. Ratner, *J. Am. Chem. Soc.*, 1997, **119**, 6575.

11 P. R. Varanasi, A. K.-Y. Jen, J. Chandrasekhar, I. N. N. Namboothiri and A. Rathna, *J. Am. Chem. Soc.*, 1996, **118**, 12443.

12 (*a*) A. R. Katritzky, in *Comprehensive Heterocyclic Chemistry*, ed. O. Meth–Cohn, Pergamon Press, Oxford, 1984, vol. 1, p. 1; (*b*) M. R. Grimmett, in *Comprehensive Heterocyclic Chemistry*, ed. O. Meth–Cohn, Pergamon Press, Oxford, 1984, vol. 1, p. 345; (*c*) G. V. Boyd, in *Comprehensive Heterocyclic Chemistry*, ed. O. Meth–Cohn, Pergamon Press, Oxford, 1984, vol. 6, p. 177; (*d*) J. V. Metzger, in *Comprehensive Heterocyclic Chemistry*, ed. O. Meth–Cohn, Pergamon Press, Oxford, 1984, vol. 6, p. 235.

13 T. L. Gilchrist, *Heterocyclic Chemistry*, John Wiley & Sons Inc., New York, 1985.

14 P. von R. Schleyer, P. K. Freeman, H. Jiao and B. Goldfuss, *Angew. Chem., Int. Ed. Engl.*, 1995, **34**, 337 and references therein.

15 C. M. Knobler, *Science*, 1990, **249**, 871.

16 M. S. Johal, A. N. Parkih, Y. Lee, J. L. Casson, L. Foster, B. I. Swanson, D. W. McBranch, Q. D. Li and J. M. Robinson, *Langmuir*, 1999, **15**, 1275.

17 (*a*) J. Glazer and A. E. Alexander, *Trans. Faraday Soc.*, 1951, **47**, 401; (*b*) B. Asgharian and D. A. Cadenhead, *J. Colloid Interface Sci.*, 1990, **134**, 522.

18 H. Chen, K.-Y. Law and D. G. Whitten, *J. Phys. Chem.*, 1996, **100**, 5949.

19 D. G. Whitten, *Acc. Chem. Res.*, 1993, **26**, 502.

20 P. Hebert, G. Baldacchino, T. Gustavsson and J. C. Mialocq, *J. Photochem. Photobiol. A*, 1994, **84**, 45.

21 (*a*) G. J. Ashwell, P. D. Jackson and W. A. Crossland, *Nature (London)*, 1994, **368**, 438; (*b*) G. J. Ashwell, G. Jefferies, C. D. George, R. Ranjan, R. B. Charters and R. P. Tatam, *J. Mater. Chem.*, 1996, **6**, 131; (*c*) G. J. Ashwell, R. C. Hargreaves, D. E. Baldwin, G. S. Bahra and C. R. Brown, *Nature (London)*, 1992, **357**, 393.